Development of Noise Budgets for the LIGO 40m IFO
SURF 2005

Ryan Kinney[1], Alan Weinstein[2⋆], Rana Adhikari[2†], Osamu Miyakawa[2†], Robert Ward[2†]
1. Department of Physics, University of Missouri-Rolla, Rolla, Mo 65409, rtk42c@umr.edu and
2. Department of Physics and Astronomy, California Institute of Technology,
Pasadena, California, 91125, ajw@ligo.caltech.edu, rana@ligo.mit.edu,
miyakawa_o@ligo.caltech.edu, rward@ligo.caltech.edu, ⋆mentors, †comentors
(Dated: June 27, 2005)

The Laser Interferometer Gravitational-wave Observatory (LIGO) represents the next advancement in the search for gravitational waves. To detect gravitational waves, the observatory must be sensitive to extremely small changes of spacetime. For this reason, all sources of noise with in LIGO must be reduced. To increase LIGO's sensitivity, a 1/100th scale prototype interferometer, 40m IFO, has been built at the California Institute of Technology to test and refine new technologies for use the second generation of LIGO, Advanced LIGO. To properly test these new technologies, the 40m IFO must also be subjected to noise reduction. However before noise reduction can be performed, the sources that contribute noise to the gravitational wave signal must be identified and quantified (budgeted). A project proposal to analyze the noise budget of the 40m IFO is presented.

INTRODUCTION

The past century has seen a revolution in the way scientists examine the universe. With the capabilities of new technology, astronomers have been able to peel away the secrets of the universe by examining the radiation produced by astrophysical sources at different frequencies in the electromagnetic spectrum. This technological *tour de force* has allowed for the study of the universe in the infrared, ultraviolet, X-ray, γ -ray, microwave, and radio wave frequency range. With each new frequency regime comes new discoveries and new questions. However, despite the wealth of information available through the electromagnetic spectrum there are limits to its capabilities. For many astrophysical phenomena, such as phenomena associated with the time before the opaque Recombination Era of the early universe, other tools are required.

Fortunately, a way around these limits exists in the form of gravitational waves (GW). Gravitational waves are implicit in Einstein's Theory of Special Relativity by its finite limit on information transfer (the speed of light) and are explicit in his Theory of General Relativity where gravity is viewed not as a force but as the curvature of space-time. Here, accelerating masses generate time-varying gravitational fields that emanate from the source as warpages of space, gravitational waves, at the speed of light in much the same way that electromagnetic waves emanate from accelerating charges [4].

Gravitational waves have many properties that distinguish them from their electromagnetic counterparts. For instance, gravitational waves are not impeded by the presence of matter. This implies that they will easily pass through interstellar gas clouds that block or scatter EM radiation and thus they will be able to directly observe the times before the Recombination Era, possibly back to the Planck Era. They can also provide information about strong field gravity sources such as black holes, neutron stars, and the processes involved in stellar core collapse (which result in supernova explosions).

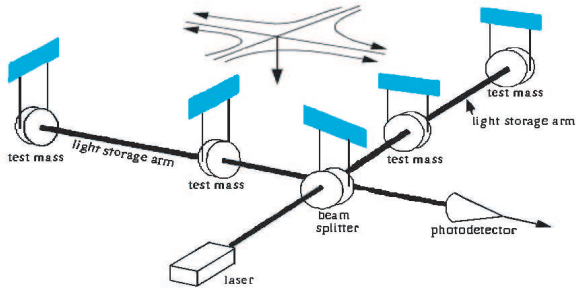

FIG. 1: Diagram showing the major LIGO components: Michelson IFO, Fabry-Perot arms, suspended test masses, beam splitter, and the anti-symmetric port photo-detector [1].

As of yet, there have been no directly detected gravitational waves. However, there is very strong indirect evidence that they exist from a binary pulsar system known as PSR1913+16. This system consists of a pulsar and a neutron star in orbit around a common center of mass. After recording two decades worth of data, it was found that the orbit of the pulsar was slowly experiencing a phase shift at exactly the rate predicted by General Relativity's gravitational waves.

To collect direct evidence, two measurement schemes are being pursued. The first system is the Resonant Mass Detector (colloquially known as the bar detector). A bar detector monitors the change of the internal vibration modes of a large, isolated metal bar due to a passing gravitational wave. The second system is the suspended mass interferometer (IFO). IFO's monitor the change in the local space-time due to a gravitational wave by sensing the change in the lengths of its arms.

The Laser Interferometer Gravitational-wave Observatory (LIGO) is the largest observatory in a world wide network of gravitational wave detectors. LIGO is a Michelson interferometer with Fabry-Perot cavities in its 4 km long arms. When a gravitational wave passes through the detector, it induces a strain, a fractional change in the lengths of the two arms, that is detected by the presence of light in the anti-symmetric port photodetector. The anti-symmetric port is dark in the absence of any strain because the light along that path has undergone destructive interference. Figure 1 shows the basic configuration for LIGO. Currently, there are two LIGO detectors (comprising one observatory) near Hanford, Washington and a observatory (with one detector) near Livingston, Louisiana. These detectors have a detection band of 40 Hz to 5 kHz for an induced strain of approximately 10^{-20} rms and a few hundred Hz band centered near 200 Hz for a strain of 10^{-21} rms. This corresponds to a displacement of only 10^{-18} m rms or 1/1000th the diameter of the nucleus of an atom over the 4 km baseline [5].

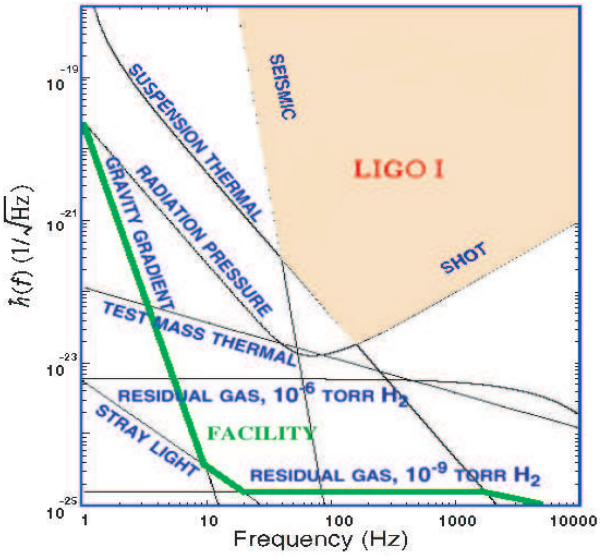

FIG. 2: The limiting noise sources for LIGO are seismic noise, suspension thermal noise, and shot noise. The shaded region represents the best possible detection range for LIGO. After years of work, LIGO has nearly achieved this detection range [2].

Due to the extreme sensitivity goal of LIGO, all possible sources of noise must be discovered and reduced, until only the "fundamental" noise sources (seismic, thermal, shot) remain. Figure 2 shows the major noise sources for LIGO and represents the best possible detection range for the current detector design. To overcome some of these sensitivity limits, a second generation of LIGO (Advanced LIGO) is being planned and will be a modification of the current design incorporating new technologies and interferometer configurations. At the California Institute of Technology, a 1/100th scale interferometer, the 40m IFO, is used as a test platform for the design, testing, and refinement of advanced technologies and techniques that will be incorporated into Advanced LIGO. As with LIGO, the 40m IFO must measure its experienced noise if it is to meet its design requirements.

OBJECTIVES

In order to measure the noise experienced by the 40 IFO, the noise must first be categorized to decipher the individual contributions of the various sources affecting the data output signals. This process is known as noise budgeting. Upon the development of a budget, noise reduction can proceed in an orderly and logical manner by selecting the most immediate noise source, wither it is the most contributing source or simply the easiest to work on, and diminishing it until the desired sensitivity is achieved. The primary objective for this project is to develop a noise budget for the 40m IFO.

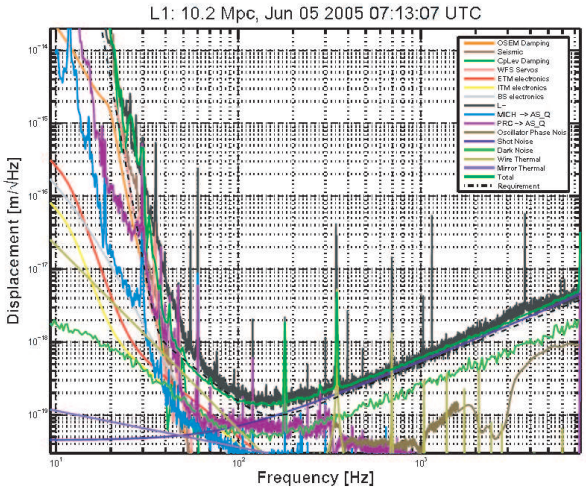

FIG. 3: The noise amplitude spectrum for the Livingston Observatory. Note the proximity of the L-(black) line to the SRD(dashed). The SRD line is the line formed by the seismic, suspension thermal, and shot noise lines from Figure 2 [3].

At the sites, budgeting is performed on a daily basis and is used to track the progress toward the SRD. Figure 3 demonstrates a noise budget for the Livingston detector on June 5, 2005. It is important to note the proximity of the L- (black) line, representing the Differential Arm (DARM, which is the channel in which a GW signal is most likely appear) signal, to the SRD (Science Requirement, dashed). This is a major accomplishment that has been aided by noise budgeting. Upon close inspection of the 30 to 70 Hz regime, there exits a gap between the total detected noise and the total expected noise. This indicates that there exists is an as yet unknown source of noise affecting the L- signal preventing it from reaching

the SRD in that frequency range. This type of revelation directly reveals the power, utility, and importance of noise budgeting.

METHODOLOGY

In order to efficiently and correctly create a noise budget for the 40m IFO, a systematic procedure must be employed. The first step in this procedure is calibration. Calibration is simply benchmarking the data output channel against a physical action with known properties. In this context, it means relating the L- (DARM) signal to the motion of the IFO end mirrors and thus to the strain experienced by the IFO. The calibration routine is divided into five subsequences. These are

1 Decide the output channel to study: the one in which the gravitational wave signal is to be detected (in our case, DARM)

2 Lock the IFO into some configuration which detects the stain caused be a passing GW

3 Drive an IFO mirror with a known oscillation while maintaining lock and determine the transfer function between the driven mirror and the output channel

4 Measure the power spectrum of the output channel

5 Iterate steps 3 and 4 for different mirrors that are relevant for the current lock

The first step in the calibration is the most crucial. The complexity of the 40m IFO requires that output channel be fully understood to ensure that the data received from it is valid. More simply, the understanding of the connection between the source and the measurement is vital to understanding the measurement. Step 2 can be achieved by locking the IFO in the Dual Recycled Michelson (DRMI) or the Fabry-Perot Michelson (FPMI) configuration and does not require a full lock of DRFPMI (which has not yet been achieved). Steps 3 and 4 are can be efficiently performed due to the comprehensive IFO control system in place at the 40m and the mathematics software package MATLAB.

The second step in developing a noise budget consists of measuring the noise produced from the various sources. This entails recording the power spectra from the output channels connected to the noise source. However if the noise source is not directly connected to the control system, then measurements with a frequency spectrum analyzer are required. Lastly, the third step consists of combining the calibrated noise and the associated transfer functions to form the total noise budget. This is accomplished with the equation

$$n^2_{output}(f) = \sum_{i=1}^{N_{source}} \left[n_{source}(f)T(Source \Rightarrow Output)(f)\right]^2 \quad (1)$$

where n_{output} is the noise experienced by the output channel, n_{source} is the noise produced by the source, and $T(Source \Rightarrow Output)$ is the transfer function relating how much noise from the source contributes to the noise in the output channel. Equation (1) expresses the assumption that the various noise sources contribute "incoherently" to the total noise measured in the output channel, DARM. However, this need not always be the case. Some noise sources could be strongly correlated or anti-correlated such that the net noise is the sum or difference and not the root-sum-square. For an explanation of transfer functions see Appendix B. With equation (1), it is possible to know if all the dominate noise sources affecting an output channel have been discovered. If there is a difference between the result of (1) and the measured value for an output channel, then repeat the calibration procedure to find the missing noise sources.

TIME LINE

- Week 2: Development of the work plan. Acquire the sites noise analysis code. Begin the first rough draft of the final paper. Learn LaTeX and MATLAB. Continue to discover the wonderful complexities of the 40m. Begin to use front-end control software. Begin to learn how to lock the IFO.

- Week 3: Understand the sites code and begin to modify them for the 40m. Identify the first few data output channels. Under supervision, excite several different mirrors to calibrate and find transfer functions between them and the output channels. If possible, start data runs for those output channels. Transmit notes to LaTeX for inclusion in the final paper. Continue working on the final paper and continue learning about LIGO.

- Week 4-9: Continue working on the initial set of output channel to ensure that their noise budget is accurate. Move on to new output channels. Transmit notes to LaTeX for inclusion in the final paper. Continue working on the final paper and continue learning about LIGO. Create final presentation.

- Week 10: Finish the noise budget (as inclusive as possible) Finish paper and Presentation. Present work.

APPENDIX A

Initial Locking Procedures for the FPMI Lock

These locking procedures were expounded by Robert Ward during his attempts to achieve a full lock on the 40m IFO. The procedure consists of four simple, although timely, steps. They are

1 Ensure electronic offsets are zero. Once so, run the script activated by the ! button on the 40m IFO Control screen (sitemap.adl)

2 Lock the arms individually

3 To maximize the gain in the arms, ensure that the beam is centered in the cavity (the arms). To center the beam, move the beam splitter (BS) in pitch and yaw.

4 Run alignment scripts

The first step is the simplest and requires the use of the main screen for the 40m IFO control software. However, the second and third steps can be very time consuming. The subroutines of step two are

A Open the necessary control screens: from a blank screen, start the MEDM software package and open IFO Align and IFO Configure screens

B Use the Restore button on the IFO Configure screen to restore either the X or Y arm first (This locks the IFO to the previously saved configuration. A configuration consists of voltage settings for the actuators that control the position and alignment of the IFO optics.)

C On the LSC main screen, ensure that the TR (transmission power) value for the restored arm (e.g. TRX) is near 1

D On the IFO Configuration screen, click the Align button for the chosen arm (The computer will perform minute adjustments to the optics pitch and yaw to maximize some quantity, e.g. the power)

E Save the current alignment states for the appropriate optics (a new configuration has been made)

F Iterate the process for the other arm

Step three involves moving the beam splitter to maximize the FP cavity gain (necessary for a strong anti-symmetric port signal for a passing GW). This can be done because the BS controls the incident angle of the laser on to the Input Test Mass of the Y (perpendicular) arm of the Michelson (ITMY). The subroutines of step three are

A Determine if the beam is incident to the central part of the End Test Mass Y (ETMY)

B Move the beam to the center of the ITMY and ETMY. This is accomplished by adjusting the pitch and yaw controls of the opposing mirror (e.g. adjusting the ITM moves the beam on the ETM and visa versa)

C Iterate the previous step until beam centered on both the ITMY and ETMY

D Align the BS to maximize power (to monitor the power readout, use the power graph of the BS)

Achieving a full lock requires many more steps than provided here. This SURF project will record the procedures as they are developed.

APPENDIX B

Feedback Control Theory

Feedback control systems have existed since antiquity. Two early examples include the flow rate controller for a water clock and the liquid level controller for a wine vessel where both control systems depend on the liquid level in a reservoir. The modern equivalent to this ancient control system is the float valve commonly found in a flush toilet. Maxwell did the first systematic studies of feedback control theory in the nineteenth century and the field experience massive growth during and after World War II [6, 7].

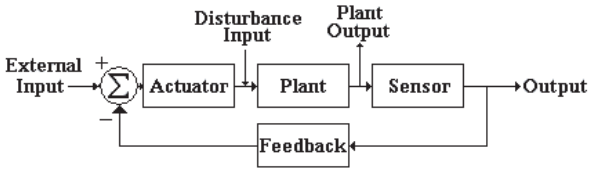

FIG. 4: A feedback control system includes the Plant, Sensors, Filter, and Actuator with the external input, disturbance input, plant output, and sensor output [6, 7]. Arrows indicate signal flow.

A *control system* is simply a device whose output follows a user controlled input and *feedback* is a strategy for control where the systems actual output is compared to the desired output, the difference used to adjust the system to achieve its desired state. For LIGO, the control system is designed to maintain the interferometer at a user defined operating configuration. This type of control system is known as a *regulator*. The major parts of a feedback cycle include the *plant*, LIGO's interferometer; the *sensor*, various devises like the photo-detectors; a compensation *filter* (where one defining feature is that the input and output have the same units), the electronics; and an *actuator*, e.g. the OSEMs [6]. The Σ is the

comparator; it compares the input from the filter against the desired input from an external source and makes a decision on how the system should respond [7]. The disturbance input, e.g. noise, is any input that would perturb the system away from its operational point, e.g. gravitational waves, and the plant output would correspond to the output of a photodiode measuring the light exiting the anti-symmetric port due to the passing of a gravitational wave.

To analyze the feedback control loop, each component of the loop is considered part of a *linear time-invariant system*. This treatment implies that the components have a linear relation between a single input and a single output. More precisely, a linear system states that if

$$s_1(t) \rightarrow g_1(t) \tag{2}$$

and

$$s_2(t) \rightarrow g_2(t) \tag{3}$$

then

$$s_1(t) + s_2(t) \rightarrow g_1(t) + g_2(t) \tag{4}$$

where $s_1(t)$ and $s_2(t)$ are inputs and $g_1(t)$ and $g_2(t)$ are outputs. Label the gain of the four components $P(s)$, $S(s)$, $F(s)$, and $A(s)$ where s is the Laplace variable, whose imaginary part is the frequency of a sinusoidally-varying signal. These are the respective transfer function for the components. A transfer function is simply viewed as a comparison of the change in output to the change in input such that

$$T(Input \Rightarrow Output) = \frac{Output}{Input}, \tag{5}$$

typically measured by using sinusoidal input signals and then measuring through a range of frequencies (swept-sine transfer function). The transfer function is the slope of the gain curve near the operating point which is where the linear approximation is valid. Fortunately, the operating point is where the system keeps itself in "lock" so it is near that value during the data runs.

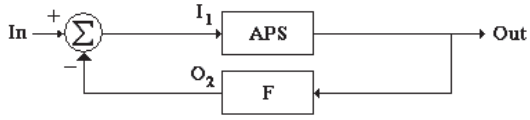

FIG. 5: This is a simple feedback loop which demonstrates the method of finding a closed loop transfer function.

From the users perspective, the transfer function for the entire IFO is a *closed loop transfer function* with *negative feedback*. In general, a closed loop transfer function is formed when the feedback filter for the system is connected while the *open loop transfer function* has the systems feedback disconnected. When examining closed systems, the open loop transfer function is found by treating the systems as open by only considering one pass through the loop. Negative feedback occurs when the output of the loop is subtracted from the external input at the comparator (another term often used for the comparator is the *summing junction*) [7]. As an example of a closed loop transfer function, consider the loop in Figure 5. In this example the external input is In; the system output is Out; APS is the transfer function for the combined system of the Actuator, Plant, and the Sensor; F is the Filter; and I_1 and O_2 are the inputs and outputs to APS and F respectively. Applying the principles of feedback theory, it is evident that

$$I_1 = In - O_2, \tag{6}$$

$$Out = APSI_1, \tag{7}$$

and

$$O_2 = FOut. \tag{8}$$

By combining the above equations and solving for Out, total system output is

$$Out = \frac{APS}{1 + FAPS} In \tag{9}$$

where the closed loop transfer function, T_{cl} is

$$T_{cl} = \frac{Out}{In} = \frac{APS}{1 + FAPS}. \tag{10}$$

The open loop transfer function $G(s)$, is simply $FAPS$ implying that the component transfer functions can be measured individually, not requiring system to be locked [6]. However, both open and closed loop transfer functions require lock because of their sensitivity to the IFO configuration. If the IFO was outside its linear range (away from the range where the linear time-invariant mathematics can be applied or, more simply, away from the locking point), then measurements of the closed and open loop transfer functions would be highly inaccurate or impossible.

When in lock, measurements of the closed and open loop transfer function can be taken by the swept-sine method. This method requires a known sinusoidal signal, e.g. from a spectrum analyzer, to be inputted in to the system and the system output to be subsequently measured. It results in a transfer function that as a measured relationship for all frequencies that can be attained by the system and, for a closed loop, has the form given by equation (10).

Both open and closed loop transfer functions experience a *gain*, the ratio of the magnitude of the signal output to magnitude of the signal input, and a phase change, given by the arctangent of the transfer function. Therefore, the gain experienced by the open loop transfer function, found by measuring the signal before the

comparator (when the comparator has a gain of 1 and causes no phase change) in the loop, is G. For example, O_2 would be the measured signal and I_1 the inputted signal for the open loop transfer function of Figure 5. Using equations (6), (7), and (8), the resulting form for the open loop transfer function is

$$T_{ol} = \frac{O_2}{I_1} = FAPS = G. \tag{11}$$

The gains experienced by the open and closed loop transfer functions are markedly different in that the close loop exhibits a *suppression* of its inputted signal. This suppression is seen by finding the transfer function between In and I_1 from equations (6), (7), and (8) giving

$$T(In \Rightarrow I_1) = \frac{1}{1+G}. \tag{12}$$

The suppression by the transfer function occurs throughout the noise spectrum. At low frequencies, the gain is large resulting in a small magnitude for the transfer function. Near the *unity gain frequency*, the magnitude rises since the denominator approaches zero. The unity gain frequency is defined as the frequency at which the gain is one and, as a consequence of the control loop at the 40m, exhibits a less than π phase shift (note $e^{i\pi} = -1$ in the complex plane and for phase angles greater than $\frac{\pi}{2}$ the complex number $e^{i\theta} = \cos\theta + i\sin\theta$ has a negative component). The gain gets smaller at frequencies higher than the unity gain frequency causing the magnitude to remain close to one.

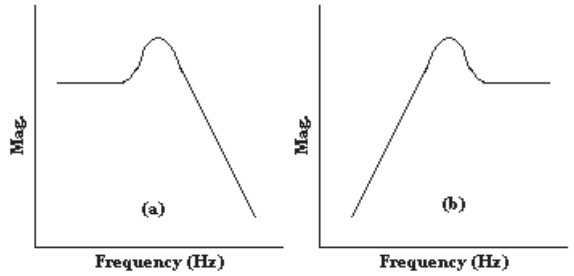

FIG. 6: (a) The resulting functional form for I_1 to O_2. (b) The form for the closed loop In to I_1 suppression. Magnitude [dB] is unit less.

A different functional form for the closed loop can be found by measuring the transfer function between In and O_2 by solving equations (6)), (7), and (8) for O_2, that is

$$T(In \Rightarrow O_2) = \frac{G}{1+G}. \tag{13}$$

The factor of G in the numerator causes the converse suppression to that produced by equation (12). Namely, the magnitude is near one at low frequencies and low at frequencies higher than the unity gain frequency. Due to the enormous number of measuring points at the 40m, these functional forms become very important in describing the transfer functions between any two data channels.

APPENDIX C

Initial Noise Budget Sources

The initial noise budget candidates were chosen because of there implementation simplicity. The initial candidates are

- Optical Shadow Sensor and Magnetic Actuator (OSEM) damping
- Seismic
- Optical Lever (OpLev) damping
- Coil Driver noise
- Analog to Digital Converter (ADC) noise
- Digital to Analog Converter (DAC) noise
- Laser noise
- Auxiliary servo noise.

Currently, not all of the candidates have direct data channels. Therefore, the output of several different channels must be combined to develop the full contribution of the noise source to the primary output channel, Differential arm (DARM, the data channel subtracting the output of the two arms to find differences in the arm output as opposed to CARM or the Common mode arm which adds the outputs to find the similarities). Furthermore, the IFO does not have all the needed equipment installed to actually measure the noise source, e.g. accelerometers are needed to measure the seismic noise contribution. The installation of the necessary equipment will commence immediately.

[1] A. Weinstein, LIGO-G02007-00-R, (Unpublished).
[2] A. Weinstein, LIGO-G000165-00-R, (Unpublished).
[3] A. Weinstein, (private communication).
[4] B. Barish, R. Weiss, Phys. Today (10) 1999.
[5] D. Coyne, "Precision Engineering in the Laser Interferometer Gravitational-wave Observatory (LIGO)", Proceedings of the 2^{nd} German-American Frontiers of Engineering Symposium, sponsored the National Academy of Engineering, Univ. of California, Irvine, April 8-10, 1999.
[6] P.R. Saulson, *Fundamentals of Interferometric Gravitational Wave Detectors*,(World Scientific, New Jersey, 1994), pp. 170-190.
[7] G.F. Franklin, J.D. Powell, A.Emami-Naeini, *Feedback Control of Dynamic Systems*, 3^{rd} Ed. (Addison-Wesley, Reading, Mass., 1994), pp.2-17.